GOLAC: An Endogenous Anion Channel of the Golgi Complex

Mark H. Nordeen,* Steven M. Jones,* Kathryn E. Howell,* and John H. Caldwell*†
Departments of *Cellular and Structural Biology and †Physiology and Biophysics, University of Colorado Health Sciences Center, Denver, Colorado 80262 USA

ABSTRACT The Golgi complex is present in every eukaryotic cell and functions in posttranslational modifications and sorting of proteins and lipids to post-Golgi destinations. Both functions require an acidic lumenal pH and transport of substrates into and by-products out of the Golgi lumen. Endogenous ion channels are expected to be important for these features, but none has been described. Ion channels from an enriched Golgi fraction cleared of transiting proteins were incorporated into planar lipid bilayers. Eighty percent of the single-channel recordings revealed the same anion channel. This channel has novel properties and has been named GOLAC (Golgi anion channel). The channel has six subconductance states with a maximum conductance of 130 pS, is open over 95% of the time, and is not voltage-gated. Significant for Golgi function, the channel conductance is increased by reduction of pH on the lumenal surface. This channel may serve two nonexclusive functions: providing counterions for the acidification of the Golgi lumen by the H^+-ATPase and removal of inorganic phosphate generated by glycosylation and sulfation of proteins and lipids in the Golgi.

INTRODUCTION

The Golgi complex modifies and sorts both proteins and lipids (Farquhar and Palade, 1998). Proteins synthesized in the endoplasmic reticulum (ER) move through the Golgi complex before arriving at their final post-Golgi destinations. These cargo proteins include both soluble (secretory) and transmembrane proteins. The major modifications are glycosylation and sulfation and, in some cells, phosphorylation of secreted proteins. Molecules exiting the Golgi are sorted into a regulated or constitutive secretory pathway or are targeted to the endosomal-lysosomal pathway. Glycosylation and sulfation of lipids also occur in the Golgi.

Structurally, the Golgi is subdivided into three regions: the *cis*, medial, and *trans* Golgi (the *trans* Golgi network, TGN), with an additional compartment that interfaces with the ER (the ERGIC or ER-Golgi intermediate *c*ompartment). It is commonly accepted that proteins transit from the ER, move through the ERGIC to the *cis* Golgi, and then move sequentially to the medial and *trans* Golgi. The lumen of the Golgi becomes progressively more acidic from *cis* to *trans*, with the *trans* Golgi being about one pH unit lower than the cytoplasm (Anderson and Pathak, 1985; Llopis et al., 1998). The enzymes resident to the *trans* Golgi (e.g., galactosyl- and sialyltransferases) are optimally active at the lower pH (Berger and Roth, 1997). In addition, the acidic environment is thought to be essential for correct sorting. For example, if NH_4Cl is used to abolish acidification, proteins are missorted in the TGN (see Kelly, 1985, for a review). Acidification of the Golgi lumen is generated by an electrogenic H^+-ATPase (Glickman et al., 1983). An anion channel was predicted to be present in the Golgi membrane to provide a counterion for the transported proton; without the counterion, a membrane potential develops that inhibits transport. Several reports indicated that a chloride conductance is present in the Golgi and is necessary to create the reduced pH of the Golgi complex (Glickman et al., 1983; Bae and Verkman, 1990; Llopis et al., 1998). These anion conductances could have been channels in transit through the Golgi and/or endogenous channels. We predicted that anion channels required for counterions for the Golgi H^+-ATPase would be both localized in and endogenous to the Golgi, because this would ensure their continued presence. Therefore, we sought to isolate and characterize endogenous Golgi channels.

Ion channels have been studied at the single-channel level not only for the plasma membrane but also for almost every intracellular organelle. However, no ion channels have been characterized that are endogenous to the Golgi complex. There are two obvious explanations for this: 1) isolating a highly enriched Golgi fraction is difficult and 2) ion channels destined for other compartments are in transit through the Golgi, and thus, endogenous channels must be separated from itinerant channels. We modified a sucrose gradient isolation procedure for rat liver Golgi (Leelavathi et al., 1970) to further enrich for Golgi markers. Rats were pretreated with cycloheximide to block protein synthesis, and under these conditions transiting proteins were cleared through the Golgi to their final destinations (Taylor et al., 1997). Analysis of the Golgi fraction isolated from control and cycloheximide-treated rat livers was performed using quantitative morphology (electron microscopy), quantitative immunoblot, and enzymatic markers of many subcellular compartments. The morphological analysis showed that more than 90% of the membrane profiles could be positively identified as Golgi stacks or cisternae. The immunoblot analysis showed enrichment in the cycloheximide

Received for publication 25 October 1999 and in final form 23 February 2000.

Address reprint requests to Dr. John H. Caldwell, Department of Cellular and Structural Biology, Box B-111, University of Colorado Health Sciences Center, 4200 E. 9th Ave., Denver, CO 80262. Tel.: 303-315-6892; Fax: 303-315-4729; E-mail: john.caldwell@uchsc.edu.

0006-3495/00/06/2918/11 $2.00

Golgi fraction of 400–700-fold for *cis*, medial, and *trans* markers and a clearance of transiting soluble and transmembrane proteins greater than 99%. This highly enriched Golgi fraction, virtually free of transiting proteins, was used for single-channel recording.

MATERIALS AND METHODS

Chemicals and solutions

Lipids for bilayer formation were a mixture of POPE (1-palmitoyl-2-oleoyl-sn-glycero-3-phosphoethanolamine) and POPS (1-palmitoyl-2-oleoyl-sn-glycero-3-[phospho-L-serine]). The bilayer was formed using a 3:1 ratio of POPE to POPS (the total lipid concentration was 20 mg/ml decane). Lipids were obtained from Avanti Polar Lipids (Alabaster, AL). Decane (99.9%) was purchased from Wiley Organics (Coshocton, OH). DIDS (4,4′-diisothiocyanatostilbene-2,2′-disulfonic acid) and other chemicals were obtained from Sigma Chemical Co. (St. Louis, MO). All recording solutions contained $MgCl_2$ (2 mM), $CaCl_2$ (1.2 mM), EGTA (1 mM), and 3-(*N*-morpholino)propanesulfonic acid (10 mM, pH 7.2) in addition to KCl.

Isolation of a Golgi fraction enriched in endogenous proteins

The fractionation protocol and characterization of the fraction (CHX SGF1) used in these experiments are presented in detail in Taylor et al. (1997). In brief, rats were pretreated with cycloheximide (50 mg/kg), and after 4 h livers were harvested. This pretreatment blocks protein synthesis and allows clearance of proteins in transit through the Golgi.

Electrophysiological recording

Planar lipid bilayers were used to study single channels in the Golgi fraction of cycloheximide-treated rat liver. Many of these experiments were carried out on the same membrane fractions used for morphological, biochemical, and immunoblot analysis (Taylor et al., 1997). The chamber used for bilayer recording was purchased from Warner Instruments (Waterbury, CT). A bilayer was formed by "painting" the lipid mixture over a 0.2-mm-diameter hole. A bilayer formed spontaneously, and when the capacitance increased to 150–200 pF, the Golgi fraction (40–65 μg protein) was added to the *cis* chamber, with stirring.

Currents are referred to as the flow of positive charge, and the *trans* chamber is defined as the electrical ground. Currents were recorded under voltage clamp, using an Axon 1B amplifier (Axon Instruments, Foster City, CA) and pClamp 5.5 software. Recordings were filtered at 1 kHz and sampled at 5 kHz. Single-channel analysis was done by two methods: 1) pClamp software (Axon Instruments) with current amplitudes set by the experimenter and threshold analysis using the 50% value method and 2) mean-variance analysis (Patlak, 1993), designed to identify and characterize subconductance states with no input from the experimenter. A mean-variance analysis program (Lischka et al., 1999) was used for dwell-time and percentage open-time calculations. Data were subsequently analyzed and plotted using Origin (Microcal). When ion replacements were performed, junction potentials were calculated using JPCalc software (written by Dr. Peter Barry, University of New South Wales, Australia). Unless indicated otherwise, the recordings were made with symmetrical 150 mM KCl solutions. Recording and ground electrodes were Ag/AgCl pellets in 1 M KCl connected to the chambers by agar bridges containing 300 mM KCl. Solutions were exchanged with eight times the chamber volume, using push-pull syringes.

RESULTS

A planar lipid bilayer was formed, and vesicles of the cycloheximide-treated Golgi fraction were added to the *cis* chamber. Channel activity was observed after spontaneous incorporation into the bilayer. When a cell is homogenized, vesicles derived from the Golgi are known to orient in their native conformation (Carey and Hirschberg, 1981; Perez and Hirschberg, 1987). Therefore, when the fraction was added to the *cis* chamber and fusion occurred, the cytoplasmic side faced the *cis* chamber and the lumenal side (inside the Golgi) faced the *trans* chamber. About one-third (46/132) of the attempts at channel incorporation resulted in single channels. The remaining two-thirds of attempted incorporations were either multiple channels or no channels. The channel described here was present in ~80% (37/46) of the single-channel recordings. The nine remaining single channels were either cation-selective channels or large-conductance anion-selective channels.

The most abundant channel was first characterized in asymmetrical KCl conditions (150 mM *cis*/10 mM *trans*) and shown to be anion selective with a reversal potential of $+22.1 \pm 2.5$ mV ($n = 10$). A channel purely selective for chloride would have had a reversal potential of +70 mV; therefore, the channel was permeable to both chloride and potassium. Calculated from the Goldman-Hodgkin-Katz equation, the chloride permeability is 2.8-fold greater than that of potassium. Two experiments using NaCl instead of KCl showed that chloride permeability was 7.7-fold greater than sodium permeability. We have named this channel GOLAC (Golgi anion channel).

Fig. 1 *A* shows typical recordings of the ion channel activity in symmetrical 150 mM KCl. A distinctive feature of the channel was the presence of five, and sometimes six, distinct steps or levels of current (designated L1–L6). Transitions from a large open state to the closed state could be observed. The current-amplitude histogram shown in Fig. 1 *B* had five peaks of approximately equal increments. A sixth level was seen for approximately a quarter of the channels. The current-voltage (*I-V*) plot for this channel (Fig. 1 *C*) was linear for all conductance levels with conductances of 33, 43, 68, 89, and 103 pS. Another example of GOLAC substate behavior is shown in Fig. 2 *A*. The lower trace in Fig. 2 *A* shows a large transition from the fully open state to the closed state. Mean-variance analysis (Fig. 2 *B*) revealed five open states and one closed state (this channel was rarely in L1 and spent most of the time in L2–L4). A composite *I-V* plot (Fig. 2 *C*, $n = 13$) shows the average currents of the L1–L5 substates. The average conductance (pS) for Levels 1–6 was 27.5 ± 3.2, 46.9 ± 3.3, 65.5 ± 2.7, 83.8 ± 2.8, 106.6 ± 5.7, and 129.6 ± 5.7 ($n = 13$ for L1–L5 and $n = 6$ for L6). The smallest open state had a conductance of 28 pS, and the difference in conductance levels between adjacent open substates was ~20 pS. It is not unusual for anion channels to exhibit substate behavior like that illustrated in

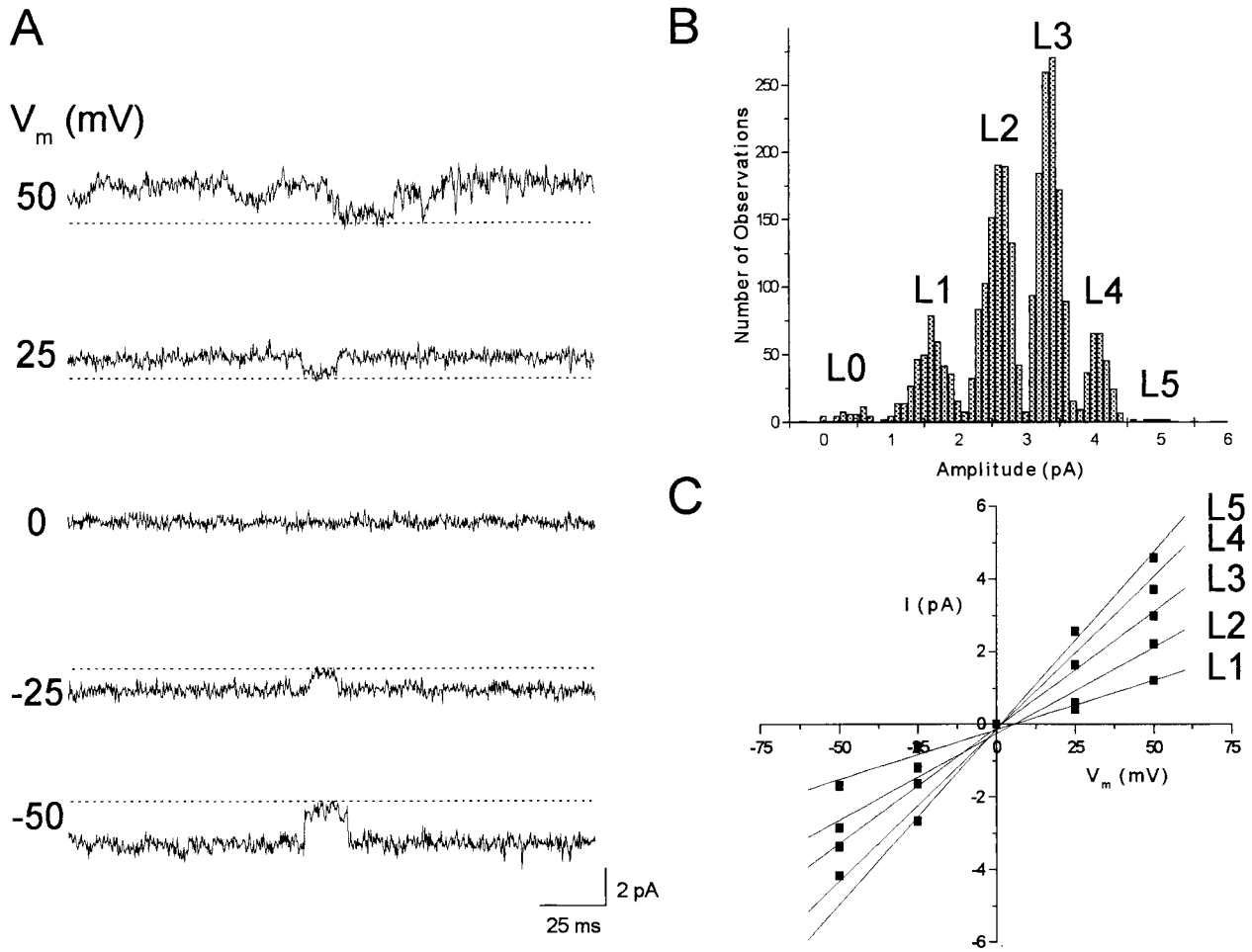

FIGURE 1 Channel conductance states in symmetrical 150 mM KCl. (*A*) Single-channel recording at different membrane potentials (*shown to the left of each trace*). The dotted line indicates the closed state. (*B*) A current-amplitude histogram (an "all-points" histogram) shows the closed state (L0) and five open states (L1–L5) at $V = +50$ mV. (*C*) Current-voltage (*I-V*) relationship for each of the five open states. The slope of each line is the conductance of that substate.

Figs. 1 and 2, but an alternative possibility is that the recording was due to multiple channels independently opening and closing.

The following observations support the conclusion that a single channel or a multipore complex exhibited this substate behavior. First, each of the GOLAC channels studied ($n = 37$) had either five or six states. We never observed single channels with only a single level having a 20-pS or a 28-pS conductance. Likewise, no channels were recorded having only two, three, or four levels composed of a combination of 20-pS and 28-pS conductances. Second, in over half (62%) of the channels, periods of rapid transitions ("bursting") among the levels were observed (Fig. 2 *D*). This behavior also suggests coordinated gating of the different levels. Bursting seemed random, i.e., no conditions (such as membrane potential) were noted that initiated, terminated, or affected the incidence of bursting. Finally, we observed rapid transitions occurring within one sample interval (200 μs) between the closed state and the upper, open states (Fig. 2 *A, arrow*). If the different levels were due to five channels rather than one channel with multiple substates, these large, rapid transitions would require simultaneous opening or closing of all channels. The probability that five channels having the kinetic properties of GOLAC substates would close simultaneously can be calculated from the mean open times of each conductance level. The mean open times (dwell times) of GOLAC substates are presented in Fig. 3 *A*. With this kinetic information, it is possible to calculate the probability that one would observe five independent channels simultaneously closing within one data sample interval (200 μs for the 5-kHz sample rate). The probability of closing within one sample interval for each state is [1 − exp(−sample interval/mean open time)] (Krouse et al., 1986; Colquhoun and Hawkes, 1995), and

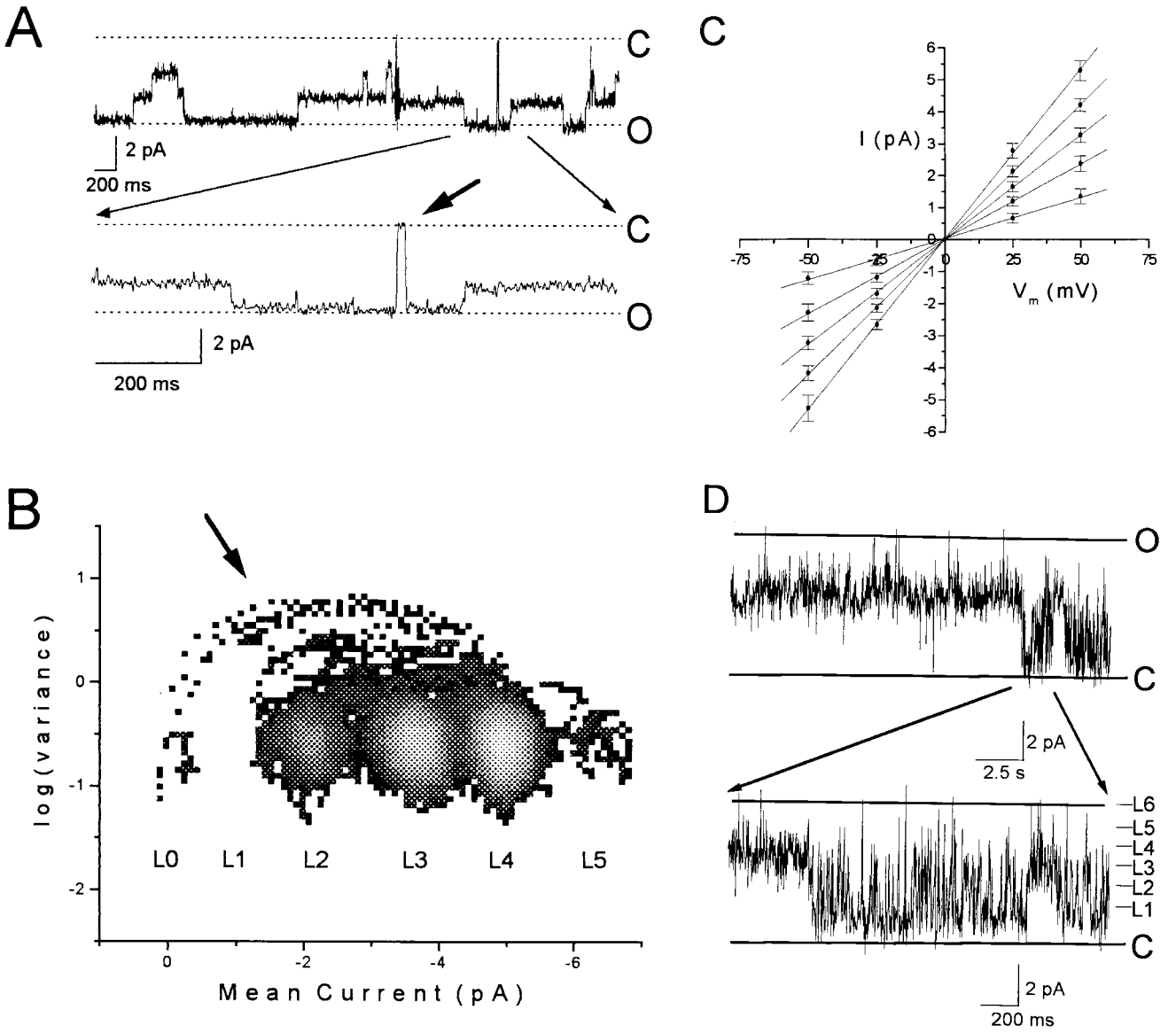

FIGURE 2 Substate behavior: current trace, mean-variance histogram, composite *I-V* plot, and bursting activity, showing substate activity and transitions from large-conducting open states to the closed state. (*A*) Current trace recorded at −50 mV (5 s of a 21.3-s recording). The lower trace is plotted at an expanded time scale to show a rapid transition (*large arrow*) from L5 to the closed state. (*B*) Mean-variance histogram of the 21.3-s recording used for *A*. The mean and variance of the current were calculated with a sliding window containing 11 data points. The *x* and *y* axes are the mean current and logarithm of the variance, respectively. The *z* axis of the histogram is the log of the number of points falling into each bin of current versus variance (current and variance were each divided into 96 bins) and is plotted as a gray scale. The background (zero points) is white. The gray scale is divided into 32 logarithmic steps (black = 1, white = 500 data points). States 2, 3, and 4 were occupied most often. Transitions between states produce an increased variance and appear as arcs between the substates (*arrow*). (*C*) Composite *I-V* plot of 13 channels. Error bars indicate the mean and standard deviation. Lines were fitted to the data by linear regression with the method of least squares. (*D*) Bursting activity. Channel switched into a bursting mode in the latter part of the record. During the burst there were short rapid transitions between states. O, fully open; C, closed. For display purposes, only a fraction of the data samples are plotted (one of every 60 data samples in the upper trace and one in every six in the expanded lower trace); consequently the larger transitions seen in the lower record are not evident in the upper record.

this is $\sim 1 \times 10^{-3}$ for many of the states. The probability of simultaneously closing is the product of the individual closing probabilities, which was calculated for several channels to be $\sim 10^{-14}$. Each data segment consisted of ~20 s of continuous recording (10^5 sample intervals), and thus the probability of observing a transition from the fully open to the closed state during the 20-s recording was $\sim 10^{-9}$. Therefore, the fact that we often observed large transitions (both opening and closing) for each GOLAC implies a coordinated gating of the states. We conclude that the mul-

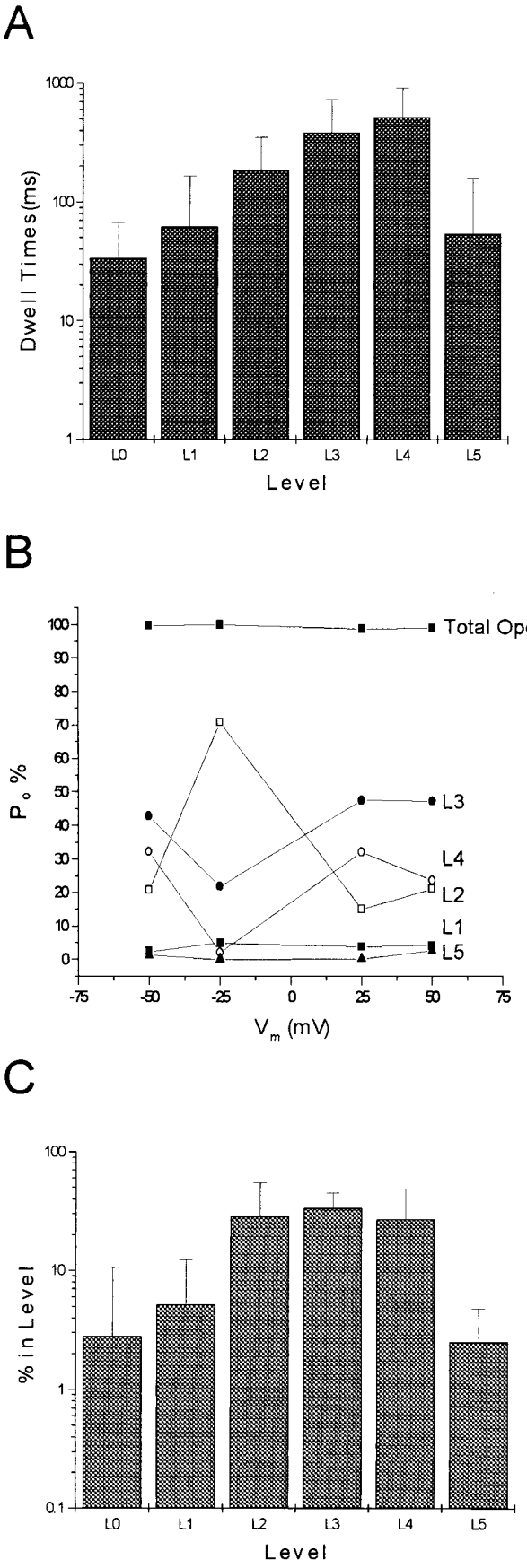

tiple substates originate from either a channel with a single pore or from a channel complex (oligo-channel) with multiple pores physically connected and coordinately gated.

Two additional properties of GOLAC are evident from Figs. 1 *A* and 2 *A*. The channel was open almost all the time, and there was no voltage dependence of channel opening. This is illustrated for one channel in Fig. 3 *B*. The open probability (P_0) for each level was the total time spent in each level, expressed as a fraction of total recording time. This channel was open (i.e., in L1–L5) more than 99% of the time at all potentials tested. P_0 showed variability for individual substates (L2–L4) at different potentials, which was most evident at −25 mV (see Fig. 3 *B*), but overall, there was a lack of voltage dependence for the total open time. Data from 13 channels were analyzed for the relative time spent in each level, and the results for $V_m = +50$ mV are plotted in Fig. 3 *C*. On average, the channel was open over 97% of the time. For both the channel in Fig. 3 *B* and for the composite data, the lowest (L1) and highest (L5) states were occupied the least.

The ability of GOLAC to discriminate between anions and cations suggests the presence of a binding site for permeant ions in the pore. One test for binding is to determine the change in conductance as a function of the anion concentration. Fig. 4 illustrates the dependence of conductance upon chloride activity. The conductance saturated as the concentration of chloride increased. The data were fit by a Michaelis-Menten relationship with a maximum conductance of 344 pS and a K_m of 380 mM Cl^-. Thus the channel has a binding site with relatively weak affinity for Cl^-.

The relative selectivity of the channel for different anions provides information about the properties of the pore and the about the molecules that are permeant. Replacement of Cl^- in the *trans* chamber with an equivalent activity of other anions produced changes in the reversal potential (Fig. 5) but little change in conductance. The permeability sequence relative to Cl^-, calculated from reversal potential changes (and corrected for liquid junction potentials), was SCN^- (2.58) > I^- (1.3) > Br^- (1.21) > Cl^- (1.0) > formate (0.34) > F^- (0.29) > phosphate (0.05). Wright and Diamond (1977) predicted selectivity sequences based on a model of electrostatic interactions in which the selectivity is determined by the difference between the hydration energy of the ion and the energy of binding to a site in the pore (an approach originally described by Eisenman). Of seven halide ion permeability sequences described by them, this is

FIGURE 3 Kinetic behavior. (*A*) Mean dwell time. Average of 13 channels at +50 mV. (*B*) Percentage of time spent in each substate as a function of membrane potential. At all membrane voltages the channel was rarely closed (99% "total open"). (*C*) Average percentage of time spent in each level: composite histogram for 13 channels. Bars are the average time (%) in each level, including the closed state (L0). The channel was closed on average 2–3% of the time. Note the logarithmic ordinate in *A* and *C*.

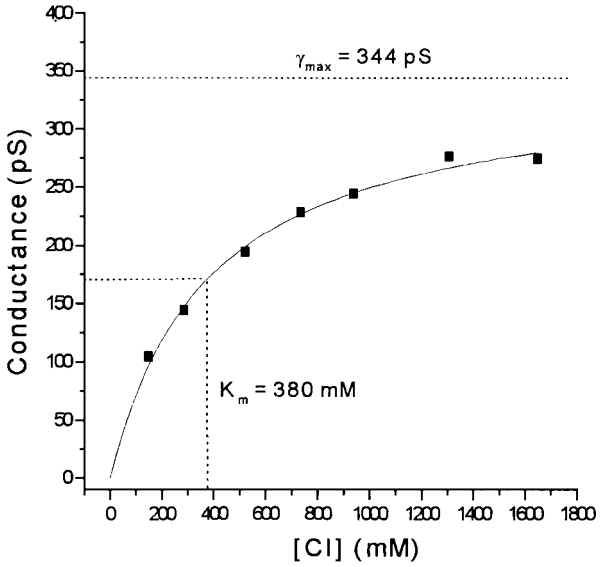

FIGURE 4 GOLAC conductance in various symmetrical Cl^- concentrations. Concentrations were changed by adding KCl to each chamber. Conductance was obtained from individual *I-V* curves and plotted as a function of Cl^- activity. Data from level 5 (the most common maximum conductance) were fitted to the Michaelis-Menten equation $\gamma = \gamma_{max}/(1 + K_m/A_{Cl-})$, where γ_{max} and K_m were varied to achieve the best fit.

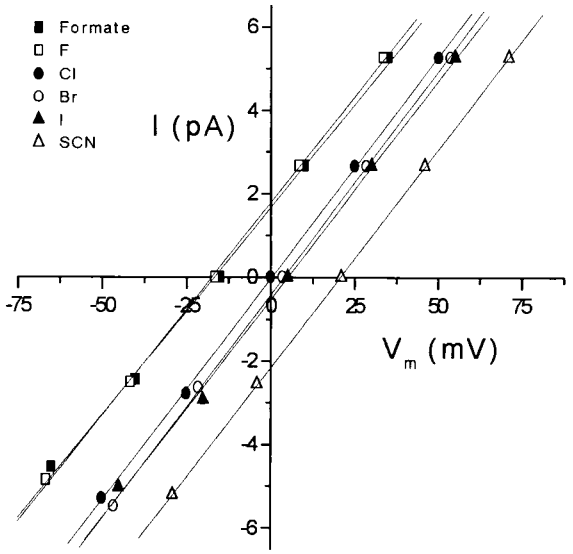

FIGURE 5 Anion selectivity. Replacement of Cl^- by various potassium salts of anions shifted the reversal potential relative to Cl^-. Potassium concentration was kept constant. Anions with greater permeability have more positive reversal potentials (reversal potential is the "zero current" intercept).

sequence 1, for which permeability is directly related to the anion size (i.e., the larger the halide ion, the greater the permeability). Sequence 1 is predicted for binding sites that are weak with a small positive charge. Methylsulfate and isethionate (each with a Stoke's diameter of 5.3 Å) were permeant, but gluconate (Stoke's diameter of 6.2 Å) was impermeant, suggesting that the pore diameter is ~5.5–6 Å. The absolute Cl^- permeability (P_{Cl}) of the pore was calculated from the current at 0 mV in asymmetrical concentrations of Cl^- (current = $P_{Cl}F([Cl^-]_{trans} - [Cl^-]_{cis})$, where F is the Faraday constant). The absolute permeability of the maximum open state for Cl^- was 1.8×10^{-13} cm^3/s.

Binding of molecules to one side or the other of the transmembrane protein often modulates the probability of opening of an ion channel. We tested several candidate molecules that had no obvious effect on the channel conductance or probability of opening. These included Ca^{+2}, cAMP, cGMP, GTPγS, and ATPγS. In addition to modulators, we also tested molecules that block channels. DIDS is known to block a wide variety of anion channels and transporters. Addition of DIDS to the *trans* chamber had no effect on Cl^- current, but addition of DIDS to the *cis* chamber blocked chloride current (Fig. 6). Moreover, DIDS in the *cis* chamber blocked the channel only for negative membrane potentials. This would be consistent with DIDS, which is doubly negatively charged, being electrically attracted to and entering the channel pore preferentially for negative membrane potentials (*cis* chamber negative relative to the *trans* chamber). At 31 μM more brief closures were evident, and this was especially notable at 125 μM. As the concentration of DIDS was increased to 500 and 1000 μM, the higher states were progressively lost (Fig. 6 *B*). Effects of DIDS are sometimes ascribed to nonspecific, covalent modifications of a channel. Two observations suggest that the block by DIDS was not due to covalent changes of GOLAC. First, the effect of DIDS was reversible. Removal of DIDS from the *cis* chamber restored channel activity. Second, with DIDS present in the *cis* chamber, chloride movement was blocked only in the *cis* to *trans* direction (i.e., for negative, but not positive membrane potentials). Thus, even with DIDS present, chloride movement from *trans* to *cis* was normal.

Because the lumen of the Golgi is reported to be about one pH unit lower than the cytoplasm and because reduced pH of the Golgi lumen is optimal for protein modification and sorting, we tested the effect of different pH values (pH 5.2–8.2) on GOLAC activity. An increase in lumenal pH to 8.2 had no effect on GOLAC conductance (pH 7.2: 106.6 ± 5.7 pS; pH 8.2: 117.0 ± 11.6 pS; level 5, $n = 3$). However, reduction of lumenal pH from 7.2 to 6.2 and 5.2 caused an increase in GOLAC conductance (Fig. 7). The conductance increased by 75% at pH 6.2 (186.5 ± 67.7 pS). In addition, the conductance increase was asymmetrical; it applied only to movement of chloride from the *cis* (cytoplasmic) to the *trans* (lumenal) chamber. Conductance was almost twofold (1.97) greater at pH 5.2 (210.3 ± 67.5 pS). Changes in pH on the cytoplasmic side had no effect. Thus the channel is pH sensitive, and conditions that mimic the native pH gradient increase conductance.

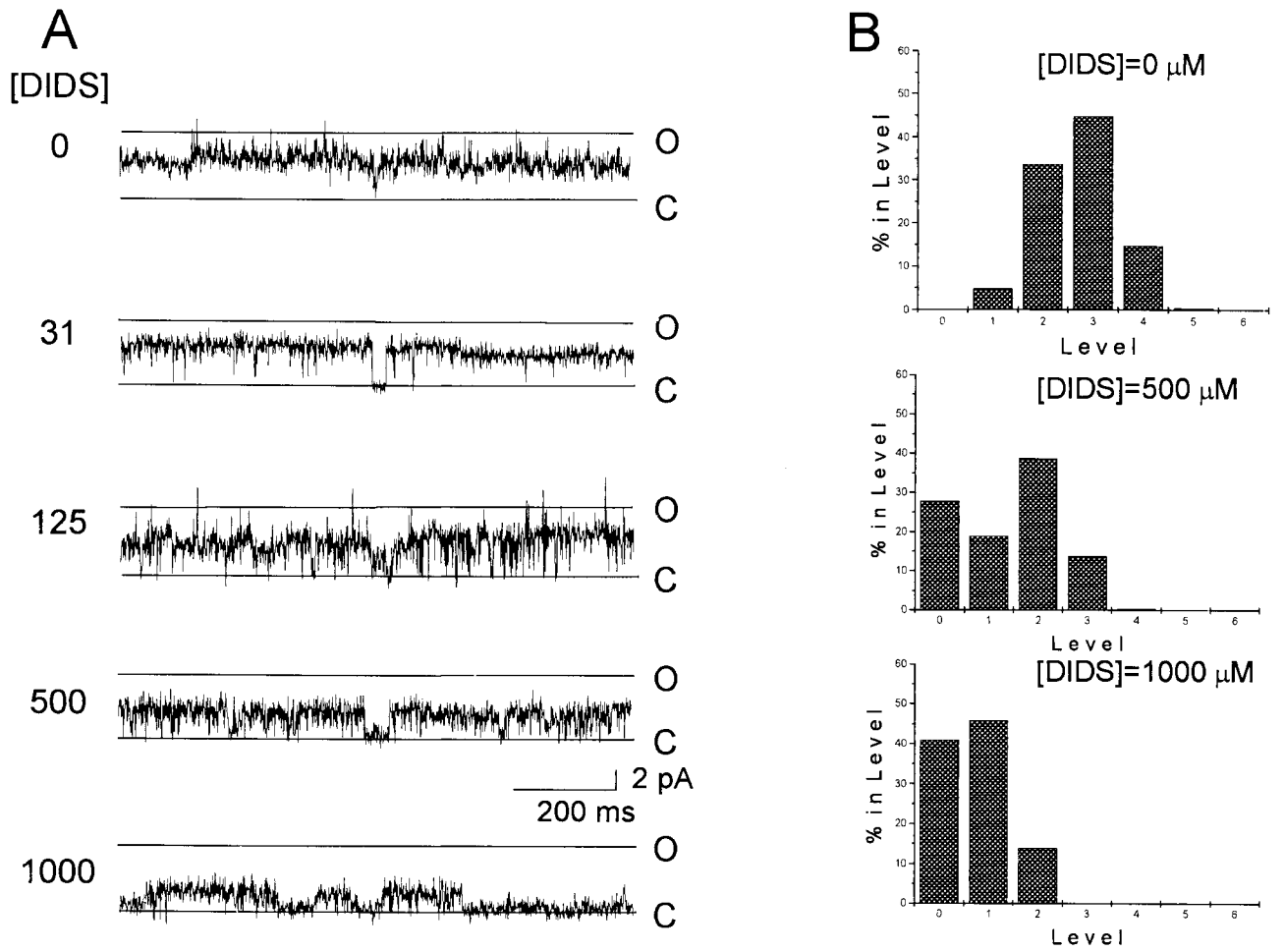

FIGURE 6 Block by DIDS. (*A*) Single-channel recordings before the addition of DIDS (*top trace*) and in the presence of DIDS (concentrations are indicated on the left in μM). DIDS was added to the *cis* (cytoplasmic) side. (*B*) Histograms of the relative time in each level at different DIDS concentrations. Note the decreased occupancy of the upper levels as DIDS concentration increased. O, fully open; C, closed.

DISCUSSION

To initiate our search for endogenous Golgi channels, it was necessary to improve standard Golgi fractionation and to eliminate proteins in transit. We enhanced the enrichment of Golgi markers and reduced contamination by adding an additional gradient centrifugation procedure to the Leelavathi Golgi fractionation protocol (Leelavathi et al., 1970). We eliminated more than 99% of proteins in transit by pretreatment with cycloheximide (Taylor et al., 1997). Together, the improved fractionation protocol resulted in ~700-fold enrichment for medial Golgi and ~400-fold enrichment for *cis* and *trans* Golgi markers. We incorporated the proteins of the enriched Golgi fraction into lipid bilayers and recorded single-channel activity. GOLAC is an anion channel with unique properties that is endogenous to the Golgi complex. Because every eukaryotic cell contains this organelle, we suggest that the Golgi channel described here carries out a basic, ubiquitous function.

GOLAC exhibited activity with subconductances that occurred in increments of 20 or 28 pS and had at least five or six open states. We conclude that GOLAC is a single-channel or multipore channel complex for the following reasons. Abrupt transitions from the maximum open state to the closed state were often observed with a frequency that was many orders of magnitude greater than would be expected for independent channels to close simultaneously. Second, bursting occurred for many of the recordings, implying coordinated opening and closing of the individual states. Third, if the states were due to separate channels, we would have expected to find channels of 20 or 28 pS or combinations thereof (e.g., one to four substates), and these were never seen.

The substate behavior could be explained by two models of the channel: 1) a single pore that undergoes multiple conformational changes, each conformation having a different conductance, or 2) multiple pores that are physically

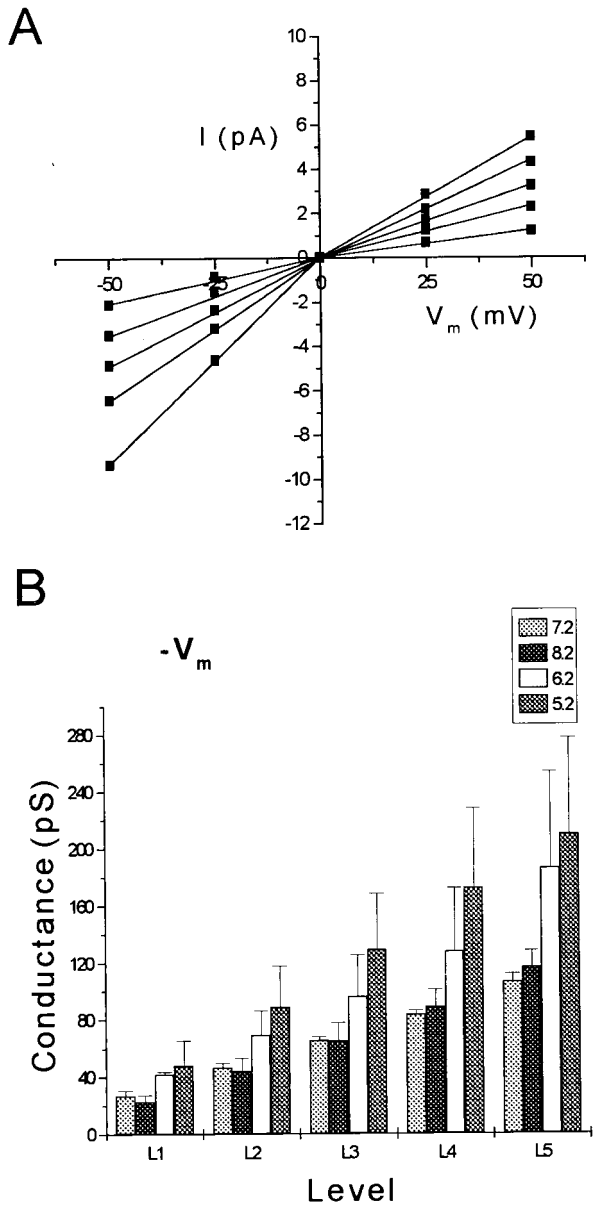

FIGURE 7 Conductance increased when lumenal pH was reduced. (*A*) Current-voltage plot at pH 6.2. Conductance increased for negative currents (movement of chloride from *cis* to *trans*). Chloride movement from *trans* to *cis* (positive currents) was unchanged. (*B*) Conductance increased for all levels for negative currents ($n = 3$) for pH 5.2 and 6.2. Conductance at pH 8.2 was not different from that at pH 7.2.

linked such that the gating is interrelated. Some anion channels (often referred to as Cl^- channels) are built with a single pore and others with multiple pores. Glycine and GABA receptors, which are ligand-gated chloride channels, have an architecture similar to that of the acetylcholine receptor with a single pore and subconductance states that are not multiples of one increment (Bormann et al., 1987). The ClC-0 chloride channel is a dimer with two equal pores that have a common closed state (both pores closed) and a state in which each pore opens and closes independently (Miller and White, 1984; Ludewig et al., 1996; Middleton et al., 1996). The fact that each open state of GOLAC differs in size from the adjacent states by ~20 pS (except for the lowest state) entices one to favor the second model. GOLAC may be a complex composed of six pores. The lowest state has a larger conductance than the other states (28 pS versus 20 pS), and one could imagine a central pore (which has a 28-pS conductance when it opens) with five identical proteins forming pores around the central one (each of the five pores having a 20-pS conductance). Other examples of channels with equal conductance states have been reported, none of which have properties identical to those of GOLAC. These include the ClC-0 chloride channel described above, a Cl^- channel from plasma membrane of epithelial cells with six open states (Krouse et al., 1986), and a Cl^- channel from brain ER with four open states (Clark et al., 1997). Despite the appeal of a multipore channel, single-pore channels can also produce substates separated by equal steps. Under certain conditions, the ryanodine receptor (a calcium release channel of the sarcoplasmic reticulum) shows four substates (Ahern et al., 1997), possibly related to the fourfold symmetry of these channels. In addition, Dani and Fox (1991) have modeled a single-pore channel and shown that equal substate increments are possible. Thus GOLAC could also be a single pore, perhaps with sixfold symmetry.

Because no cell fractionation procedure results in the isolation of a "pure" organelle, GOLAC could potentially come from a contaminant in the Golgi fraction. Both morphological evidence and the presence of marker proteins demonstrate minimal amounts of ER and lysosomal contamination in the Golgi fraction used to characterize GOLAC (Taylor et al., 1997). Confirmation that the channel resides in the Golgi can only be accomplished by localization studies. This can be carried out with an antibody against GOLAC or with expression of GOLAC cDNA fused to GFP or an epitope tag. However, there are three compelling reasons to believe that GOLAC is a Golgi channel. The strongest argument that GOLAC is a Golgi channel is that no other channel with the properties of GOLAC has previously been described by others in recordings from endoplasmic reticulum (Simon and Blobel, 1991; Morier and Sauve, 1994; Duncan et al., 1997; Eliassi et al., 1997; Schmid et al., 1988), sarcoplasmic reticulum (Townsend and Rosenberg, 1995; Hals et al., 1989; Rousseau, 1989), or lysosomal fractions (Tilly et al., 1992). In addition, none of the single channels recorded from liver (the tissue source for our studies) were similar to GOLAC (plasma membranes (Henderson et al., 1989; Sellinger et al., 1992), organelles (mitochondria; Bowen et al., 1985; Costa et al., 1991; Selwyn et al., 1990), and peroxisomes (Labarca et al., 1986; Lemmens et al., 1989)). Second, the enrichment for Golgi markers in the cycloheximide Golgi fraction is orders of

magnitude greater than for any other organelle. Finally, GOLAC was the most prevalent channel (36/47) of the enriched Golgi fraction.

The properties of GOLAC do not clearly place it in one of the previously described classes of anion channels. There are three known major families of anion channels: 1) The ABC (ATP binding cassette) family includes the CFTR (cystic fibrosis transmembrane regulator) and multidrug resistance channels. These channels have multiple modulatory regions, and both ATP (direct binding) and phosphorylation regulate conductance. 2) Ligand-gated channels, e.g., GABA and glycine receptors, require ligand binding to open. 3) The voltage-gated chloride channel (ClC) family includes at least nine related genes in mammals (Jentsch, 1993; Brandt and Jentsch, 1995; Jentsch et al., 1999). The lack of nucleotide effects and the absence of a requirement for a ligand for opening argue against membership in the ABC and ligand-gated families of channels. The ClC channels have some features that suggest that they may be related to GOLACs. The yeast genome contains only one gene (GEF1) with homology to the ClC channels, and the GEF1 protein has been localized to the medial Golgi (Schwappach et al., 1998). Several ClC cDNAs have been isolated that cannot be expressed on the plasma membrane in *Xenopus* oocytes. Of several possible explanations (e.g., missing a subunit of a heteromultimer), one explanation that has been proposed is that these channels are targeted not to the plasma membrane but to intracellular organelles (Brandt and Jentsch, 1995). The ClC channels that are possibly intracellular (Jentsch, 1993; Jentsch et al., 1999) are ClC-3 (but see Duan et al., 1997), ClC-6 (Brandt and Jentsch, 1995; Buyse et al., 1998), and ClC-7 (Brandt and Jentsch, 1995). Another ClC channel (ClC-5) is found in both early endosomes and on the plasma membrane and appears to colocalize with the H^+-ATPase in the proximal tubule of the kidney (Gunther et al., 1998). However, ClC-5 is not ubiquitously expressed and is expressed at a low level in the liver (the tissue source for GOLAC recordings). There are a number of features that are different between ClC channels and GOLAC, e.g., voltage dependence, the relative selectivity for different anions, and the magnitude of the conductance. Some of these differences could be due to factors missing in the bilayer recordings, and GOLAC could be a member of the ClC family. Alternatively, GOLAC may be a member of a family not yet described.

Hypotheses

We suggest two possible roles for GOLAC that are not mutually exclusive. First, the channel acts to prevent charge accumulation due to transport (by an electrogenic H^+-ATPase) of H^+ into the Golgi. Thus it is necessary for acidification of the Golgi. There are several experiments that indicate that an anion channel is present and important for Golgi acidification (Glickman et al., 1983; Bae and Verkman, 1990) (see al-Awqati, 1995, for a review). The high probability of being open and the increased conductance of GOLAC when the lumenal side is acidic are consistent with this hypothesis. The second hypothesis is that GOLAC could act as a phosphate transporter to remove phosphate from the Golgi lumen. Although phosphate is only ~1/20 as permeant as chloride (determined by the shift in reversal potential after replacement of Cl^- by P_i in the *trans* chamber), its flux would still be orders of magnitude greater than that of most transporters. Glycosylation of newly synthesized proteins and lipids is a major role of the Golgi. It is estimated that there are over 200 glycosyltransferases and glycosidases involved in the biosynthesis of known glycans (Varki, 1998), and each catalyzes a different carbohydrate linkage. In general, each sugar added to protein or lipid in the Golgi is transferred from a nucleotide diphosphate sugar (e.g., UDP-sugar). After the sugar transfer, the free UDP is cleaved by a phosphatase, keeping the overall reaction from going backward by generating UMP and free phosphate. The UMP drives the antiporter that brings in UDP-sugar and thereby exits the lumen. Thus an inorganic phosphate is generated for each sugar added to proteins and lipids in the Golgi (reviewed by Hirschberg et al., 1998). Similarly, posttranslational addition of sulfate to proteins, lipids, and carbohydrates occurs in the Golgi, and each added sulfate is accompanied by the generation of an inorganic phosphate (Huttner and Baeuerle, 1988).

A mechanism for the removal of phosphate is currently unknown. If, as is true for anion channels in general, GOLAC is more permeant to singly charged phosphate ($H_2PO_4^-$) than to doubly charged phosphate (HPO_4^{2-}), the low pH in the Golgi lumen could be responsible for producing an efflux of phosphate through GOLAC. At an acidic pH, inorganic phosphate (P_i) will bind two H^+ and be primarily singly charged. When it exits the Golgi and encounters a shift of one pH unit in the cytoplasm (from ~6 to 7), the phosphate will lose a proton and become doubly charged and less permeant. This would result in a unidirectional movement of P_i (and of H^+) from the lumen to the cytoplasm. This provides a novel explanation for the requirement of an acidic Golgi lumen, namely that an acidic lumen makes the phosphate permeant through GOLAC and is essential for the removal of phosphate.

The high probability that GOLAC is open implies that the membrane potential of the Golgi will be small. A recent report using in vivo imaging of GFP galactosyltransferase showed that the Golgi membrane potential with normal Cl^- is small or nonexistent (Llopis et al., 1998). Thus P_i movement via GOLAC would depend mainly on the concentration gradient. Although the free P_i concentration in the cytoplasm of liver cells is ~2 mM (Tanaka et al., 1989), the intralumenal P_i concentration is not known. In the Appendix we estimate that the rate of generation of P_i in the Golgi lumen of a single hepatocyte due to protein glycosylation would produce a 1 mM/s increase in $[P_i]$. Given these

assumptions, 100 GOLAC channels would be sufficient to transport P_i out of the lumen. In summary, both hypotheses we propose are plausible. GOLAC could be the basis for Cl^- movement into the lumen (to provide the electrical balance for the transport of H^+) as well as movement of inorganic phosphate out of the lumen.

APPENDIX: ESTIMATE OF THE RATE OF PRODUCTION OF P_i IN THE GOLGI COMPLEX DUE TO GLYCOSYLATION AND SULFATION OF PROTEINS AND LIPIDS

To estimate the rate of production of P_i in the rat liver Golgi complex, we need to know 1) the rate of production of glycosylated and sulfated proteins and lipids in a single hepatocyte and 2) the average number of monosaccharides and sulfates added to these proteins and lipids in the Golgi. To translate this rate of P_i generation per cell into a rate of change in concentration in the lumen of the entire Golgi stack, the intralumenal volume of the Golgi ribbon must be estimated. At the outset, we recognize that this will undoubtedly be a rough estimate, given the lack of detailed information about the rates of synthesis and variation in the amount of glycosylation and sulfation of each protein and lipid synthesized by the hepatocyte.

Approximately half the protein secreted by the liver is albumin (which is not glycosylated), and the other half is composed of more than 100 proteins that are glycosylated and a few that are also sulfated. The rate of production of albumin by the rat liver has been reported to be 0.75 mg/g liver/h (Morgan, 1983). Therefore, we assume that the rate of glycosylated protein synthesis is equivalent to this rate, and if we assume that the average molecular mass of these proteins is 50 kDa, the liver secretes 9×10^{15} glycosylated molecules/g liver/h. Hepatocytes constitute ~80% of the liver (Blouin, 1983), and if we assume that each hepatocyte is 25 μm in diameter with a specific density of 1.06, 1 g of liver contains 1×10^8 hepatocytes. Therefore, each hepatocyte secretes 9×10^7 glycosylated proteins/h or $\sim 2.5 \times 10^4$ glycosylated proteins/s. We assume that the average number of monosaccharides added to N-linked glycans in the Golgi per protein is 20 (based on a range of 2–20% of protein molecular weight contributed by carbohydrates). Thus, as a consequence of protein glycosylation, each hepatocyte generates 5×10^5 P_i/s in the Golgi complex. The intralumenal volume of the Golgi complex of the rat NRK cell line has recently been measured and is 0.8 μm^3 (Ladinsky et al., 1999). With this value for the volume of the Golgi stack, the concentration of P_i within the Golgi increases by ~1 mM/s if there is no means of removing the P_i.

How many GOLAC proteins would be required for this P_i to exit? If we assume that the membrane potential is close to zero (Llopis et al., 1998), the flux is described by Fick's law (flux = permeability × concentration gradient). We have determined that P_i permeability is 1/20 that of Cl (we have measured P_{Cl} to be 1.8×10^{-13} cm^3/s). Rat liver cytosolic [P_i] has been calculated to be 2 mM from studies with phosphorus magnetic resonance spectroscopy (Tanaka et al., 1989). The intralumenal [P_i] is unknown and is a function of how many GOLACs are present in the Golgi. At steady state, the rate of production of P_i is balanced by its rate of removal. If we arbitrarily assume that the steady-state [P_i] in the Golgi lumen is 1 mM greater than that of the cytoplasm (i.e., 3 mM), this concentration gradient will create a flux of 5×10^3 P_i/s through a single GOLAC. With these assumptions, we conclude that 100 channels would be sufficient to keep up with the generation of P_i. A greater (or lesser) number of channels would imply a lower (or higher) concentration gradient to generate the same efflux.

In this analysis we have neglected both the contribution of lipid glycosylation and the sulfation of proteins and lipids. These would of course increase the P_i formed and the number of channels required. We assume that the majority of protein synthesis is for secreted proteins, and lipids secreted by the hepatocyte are generally not glycosylated. Likewise, we assume that sulfation reactions are at most a few percent of the protein glycosylation. Therefore, our estimate is that these numbers are small and would add 5% or less to the estimate. We have also neglected a variety of potential complications, primarily because of the lack of information. For example, we have assumed that the Golgi lumen volume is constant and uniform, which is undoubtedly not correct. We have also not considered the possibility that channels in transit contribute to the removal of phosphate because it is not clear which channels would be present or if they are functional in the Golgi. Thus this estimate will certainly undergo revisions in the future.

We thank Dr. Diego Restrepo for the Levels program for mean variance analysis.

This work was supported by National Institutes of Health grants GM42629 (KEH) and GM59987 (JHC and KEH).

REFERENCES

Ahern, G. P., P. R. Junankar, and A. F. Dulhunty. 1997. Subconductance states in single-channel activity of skeletal muscle ryanodine receptors after removal of FKBP12. *Biophys. J.* 72:146–162.

al-Awqati, Q. 1995. Chloride channels of intracellular organelles. *Curr. Opin. Cell Biol.* 7:504–508.

Anderson, R. G., and R. K. Pathak. 1985. Vesicles and cisternae in the trans Golgi apparatus of human fibroblasts are acidic compartments. *Cell.* 40:635–643.

Bae, H. R., and A. S. Verkman. 1990. Protein kinase A regulates chloride conductance in endocytic vesicles from proximal tubule. *Nature.* 348: 637–639.

Berger, E. G., and J. Roth. 1997. The Golgi Apparatus. Birkhäuser Verlag, Basel.

Blouin, A. 1983. Anatomy of the liver. *In* Plasma Protein Secretion by the Liver. H. Glaumann, T. Peters, Jr., and C. Redman, editors. Academic Press, New York. 31–52.

Bormann, J., O. P. Hamill, and B. Sakmann. 1987. Mechanism of anion permeation through channels gated by glycine and gamma-aminobutyric acid in mouse cultured spinal neurones. *J. Physiol. (Lond.).* 385: 243–286.

Bowen, K. A., K. Tam, and M. Colombini. 1985. Evidence for titratable gating charges controlling the voltage dependence of the outer mitochondrial membrane channel, VDAC. *J. Membr. Biol.* 86:51–59.

Brandt, S., and T. J. Jentsch. 1995. ClC-6 and ClC-7 are two novel broadly expressed members of the CLC chloride channel family. *FEBS Lett.* 377:15–20.

Buyse, G., D. Trouet, T. Voets, L. Missiaen, G. Droogmans, B. Nilius, and J. Eggermont. 1998. Evidence for the intracellular location of chloride channel (CIC)-type proteins: co-localization of CIC-6a and CIC-6c with the sarco/endoplasmic-reticulum Ca^{2+} pump SERCA2b. *Biochem. J.* 330:1015–1021.

Carey, D. J., and C. B. Hirschberg. 1981. Topography of sialoglycoproteins and sialyltransferases in mouse and rat liver Golgi. *J. Biol. Chem.* 256:989–993.

Clark, A. G., D. Murray, and R. H. Ashley. 1997. Single-channel properties of a rat brain endoplasmic reticulum anion channel. *Biophys. J.* 73: 168–178.

Colquhoun, D., and A. G. Hawkes. 1995. The principles of the stochastic interpretation of ion channel mechanisms. *In* Single Channel Recording. B. Sakmann and E. Neher, editors. Plenum Press, New York. 397–482.

Costa, G., K. W. Kinnally, and J. J. Diwan. 1991. Patch clamp analysis of a partially purified ion channel from rat liver mitochondria. *Biochem. Biophys. Res. Commun.* 175:305–310.

Dani, J. A., and J. A. Fox. 1991. Examination of subconductance levels arising from a single ion channel. *J. Theor. Biol.* 153:401–423.

Duan, D., C. Winter, S. Cowley, J. R. Hume, and B. Horowitz. 1997. Molecular identification of a volume-regulated chloride channel. *Nature.* 390:417–421.

Duncan, R. R., P. K. Westwood, A. Boyd, and R. H. Ashley. 1997. Rat brain p64H1, expression of a new member of the p64 chloride channel protein family in endoplasmic reticulum. *J. Biol. Chem.* 272: 23880–23886.

Eliassi, A., L. Garneau, G. Roy, and R. Sauve. 1997. Characterization of a chloride-selective channel from rough endoplasmic reticulum membranes of rat hepatocytes: evidence for a block by phosphate. *J. Membr. Biol.* 159:219–229.

Farquhar, M. G., and G. E. Palade. 1998. The Golgi apparatus: 100 years of progress and controversy. *Trends Cell Biol.* 8:2–10.

Glickman, J., K. Croen, S. Kelly, and Q. al-Awqati. 1983. Golgi membranes contain an electrogenic H^+ pump in parallel to a chloride conductance. *J. Cell Biol.* 97:1303–1308.

Gunther, W., A. Luchow, F. Cluzeaud, A. Vandewalle, and T. J. Jentsch. 1998. ClC-5, the chloride channel mutated in Dent's disease, colocalizes with the proton pump in endocytotically active kidney cells. *Proc. Natl. Acad. Sci. USA.* 95:8075–8080.

Hals, G. D., P. G. Stein, and P. T. Palade. 1989. Single channel characteristics of a high conductance anion channel in "sarcoballs." *J. Gen. Physiol.* 93:385–410.

Henderson, R. M., J. Graf, and J. L. Boyer. 1989. Inward-rectifying potassium channels in rat hepatocytes. *Am. J. Physiol.* 256: G1028–G1035.

Hirschberg, C. B., P. W. Robbins, and C. Abeijon. 1998. Transporters of nucleotide sugars, ATP, and nucleotide sulfate in the endoplasmic reticulum and Golgi apparatus. *Annu. Rev. Biochem.* 67:49–69.

Huttner, W. B., and P. A. Baeuerle. 1988. Protein sulfation on tyrosine. *Mod. Cell Biol.* 6:97–140.

Jentsch, T. J. 1993. Chloride channels. *Curr. Opin. Neurobiol.* 3:316–321.

Jentsch, T. J., T. Friedrich, A. Schriever, and H. Yamada. 1999. The CLC chloride channel family. *Pflugers Arch. Eur. J. Physiol.* 437:783–795.

Kelly, R. B. 1985. Pathways of protein secretion in eukaryotes. *Science.* 230:25–32.

Krouse, M. E., G. T. Schneider, and P. W. Gage. 1986. A large anion-selective channel has seven conductance levels. *Nature.* 319:58–60.

Labarca, P., D. Wolff, U. Soto, C. Necochea, and F. Leighton. 1986. Large cation-selective pores from rat liver peroxisomal membranes incorporated to planar lipid bilayers. *J. Membr. Biol.* 94:285–291.

Ladinsky, M. S., D. N. Mastronarde, J. R. McIntosh, K. E. Howell, and L. A. Staehelin. 1999. Golgi structure in three dimensions: functional insights from the normal rat kidney cell. *J. Cell Biol.* 144:1135–1149.

Leelavathi, D. E., L. W. Estes, D. S. Feingold, and B. Lombardi. 1970. Isolation of a Golgi-rich fraction from rat liver. *Biochim. Biophys. Acta.* 211:124–138.

Lemmens, M., K. Verheyden, P. Van Veldhoven, J. Vereecke, G. P. Mannaerts, and E. Carmeliet. 1989. Single-channel analysis of a large conductance channel in peroxisomes from rat liver. *Biochim. Biophys. Acta.* 984:351–359.

Lischka, F. W., M. M. Zviman, J. H. Teeter, and D. Restrepo. 1999. Characterization of inositol-1,4,5-trisphosphate-gated channels in the plasma membrane of rat olfactory neurons. *Biophys. J.* 76:1410–1422.

Llopis, J., J. M. McCaffery, A. Miyawaki, M. G. Farquhar, and R. Y. Tsien. 1998. Measurement of cytosolic, mitochondrial, and Golgi pH in single living cells with green fluorescent proteins. *Proc. Natl. Acad. Sci. USA.* 95:6803–6808.

Ludewig, U., M. Pusch, and T. J. Jentsch. 1996. Two physically distinct pores in the dimeric ClC-0 chloride channel. *Nature.* 383:340–343.

Middleton, R. E., D. J. Pheasant, and C. Miller. 1996. Homodimeric architecture of a ClC-type chloride ion channel. *Nature.* 383:337–340.

Miller, C., and M. M. White. 1984. Dimeric structure of single chloride channels from *Torpedo electroplax*. *Proc. Natl. Acad. Sci. USA.* 81: 2772–2775.

Morgan, E. H. 1983. Synthesis and secretion of transferrin. *In* Plasma Protein Secretion by the Liver. H. Glaumann, T. Peters, Jr., and C. Redman, editors. Academic Press, New York. 331–355.

Morier, N., and R. Sauve. 1994. Analysis of a novel double-barreled anion channel from rat liver rough endoplasmic reticulum. *Biophys. J.* 67: 590–602.

Patlak, J. B. 1993. Measuring kinetics of complex single ion channel data using mean-variance histograms. *Biophys. J.* 65:29–42.

Perez, M., and C. B. Hirschberg. 1987. Transport of sugar nucleotides into the lumen of vesicles derived from rat liver rough endoplasmic reticulum and Golgi apparatus. *Methods Enzymol.* 138:709–715.

Rousseau, E. 1989. Single chloride-selective channel from cardiac sarcoplasmic reticulum studied in planar lipid bilayers. *J. Membr. Biol.* 110:39–47.

Schmid, A., H. Gogelein, T. P. Kemmer, and I. Schulz. 1988. Anion channels in giant liposomes made of endoplasmic reticulum vesicles from rat exocrine pancreas. *J. Membr. Biol.* 104:275–282.

Schwappach, B., S. Stobrawa, M. Hechenberger, K. Steinmeyer, and T. J. Jentsch. 1998. Golgi localization and functionally important domains in the NH_2 and COOH terminus of the yeast CLC putative chloride channel Gef1p. *J. Biol. Chem.* 273:15110–15118.

Sellinger, M., S. A. Weinman, R. M. Henderson, A. Zweifach, J. L. Boyer, and J. Graf. 1992. Anion channels in rat liver canalicular plasma membranes reconstituted into planar lipid bilayers. *Am. J. Physiol.* 262: G1027–G1032.

Selwyn, M. J., C. L. Ng, and H. L. Choo. 1990. Calcium ion activation of the anion-conducting channel in the rat liver mitochondrial inner membrane. *FEBS Lett.* 269:205–208.

Simon, S. M., and G. Blobel. 1991. A protein-conducting channel in the endoplasmic reticulum. *Cell.* 65:371–380.

Tanaka, A., B. Chance, and B. Quistorff. 1989. A possible role of inorganic phosphate as a regulator of oxidative phosphorylation in combined urea synthesis and gluconeogenesis in perfused rat liver. A phosphorus magnetic resonance spectroscopy study. *J. Biol. Chem.* 264:10034–10040.

Taylor, R. S., S. M. Jones, R. H. Dahl, M. H. Nordeen, and K. E. Howell. 1997. Characterization of the Golgi complex cleared of proteins in transit and examination of calcium uptake activities. *Mol. Biol. Cell.* 8:1911–1931.

Tilly, B. C., G. M. Mancini, J. Bijman, P. G. van Gageldonk, C. E. Beerens, R. J. Bridges, H. R. de Jonge, and F. W. Verheijen. 1992. Nucleotide-activated chloride channels in lysosomal membranes. *Biochem. Biophys. Res. Commun.* 187:254–260.

Townsend, C., and R. L. Rosenberg. 1995. Characterization of a chloride channel reconstituted from cardiac sarcoplasmic reticulum. *J. Membr. Biol.* 147:121–136.

Varki, A. 1998. Factors controlling the glycosylation potential of the Golgi apparatus. *Trends Cell Biol.* 8:34–40.

Wright, E. M., and J. M. Diamond. 1977. Anion selectivity in biological systems. *Physiol. Rev.* 57:109–156.